01 Jul 1994

Analysis of Radiation from an Open-Ended Coaxial Line into Stratified Dielectrics

Sasan Bakhtiari

Stoyan I. Ganchev

R. Zoughi
Missouri University of Science and Technology, zoughi@mst.edu

Recommended Citation

S. Bakhtiari et al., "Analysis of Radiation from an Open-Ended Coaxial Line into Stratified Dielectrics," *IEEE Transactions on Microwave Theory and Techniques*, vol. 42, no. 7, pp. 1261-1267, Institute of Electrical and Electronics Engineers (IEEE), Jul 1994.
The definitive version is available at https://doi.org/10.1109/22.299765

Analysis of Radiation from an Open-Ended Coaxial Line into Stratified Dielectrics

Sasan Bakhtiari, *Member, IEEE,* Stoyan I. Ganchev, *Senior Member, IEEE,* and Reza Zoughi, *Senior Member, IEEE*

***Abstract*—Radiation from an open-ended coaxial transmission line into an N-layer dielectric medium is studied in application to nondestructive evaluation of materials. Explicit formulations for two cases of layered media, one terminated into an infinite half-space and the other into a conducting sheet are addressed in general form. In the theoretical derivations it is assumed that only the fundamental TEM mode propagates inside the coaxial line. The terminating admittance of the line is then formulated using the continuity of the power flow across the aperture. The admittance expressions for specific cases of two-layer dielectric composite with generally lossy dielectric properties, and a two-layer composite backed by a conducting sheet are presented and inspected explicitly. The numerical results of the aperture admittance formulation are discussed and compared with the available infinite half-space model which had been experimentally verified.**

I. Introduction

THE use of an open-ended coaxial line as a sensor for measurement of complex dielectric properties of materials at microwave frequencies has received considerable attention [1]–[13]. Open-ended coaxial sensors allow operation in a wide band of frequencies while requiring a relatively small sensing area. Open-ended transmission line methods such as open-ended waveguides and coaxial lines are inherently nondestructive, and offer *in situ* measurement of dielectric properties. They may render valuable information about the constituency of dielectric mixtures, accurate thickness of thin dielectric slabs, presence of disbonds and delaminations in layered media [14]–[17]. These features have rendered open-ended transmission line sensors as versatile sensing/interrogating tools in contemporary biomedical, microwave engineering, and microwave nonintrusive applications.

Several approaches are commonly sighted for modeling the terminating admittance of an open-ended coaxial line. The prevalent analytical procedures used in practice for dielectric properties estimation are limited to electrically small apertures or low operating frequencies allowing lumped parameter approach or quasi-static approximation [1], [3]. Furthermore, they usually pertain to an aperture terminated into an infinite dielectric half-space, thus, not addressing the problem of finite thickness dielectrics. Mosing *et al.* considers a more rigorous formulation which takes into account higher order modes, but this computationally intensive solution only deals with the case of an infinite half-space [2]. Concise general formulation for open-ended coaxial lines terminated by multilayered dielectric media backed or unbacked by a conducting sheet which can be implemented without considerable computing resources has numerous applications. The available formulations for multilayered dielectrics either use a lumped parameter approach, or a quasi-static approximation rendering frequency independent solutions [18], [19].

In this paper a general formulation for the radiation from an open-ended coaxial transmission line into a multilayered dielectric composite backed or unbacked with a conducting sheet is considered. Integral Hankel transforms are employed to construct the field solutions in the layered media. Only the fundamental TEM mode is considered to be propagating inside the coaxial line. The terminating aperture admittance in presence of multilayered dielectric is constructed by applying complex Poynting's theorem at the aperture cross section, and requiring the continuity of power flow. Consequently, solution of the boundary value problem renders a set of recurrence relations allowing for construction of solution for multilayered geometries. Explicit admittance expressions for two frequently encountered practical cases of single dielectric slab backed by an infinite dielectric half-space, and a two layer dielectric backed by a conducting sheet are presented and examined in detail. In all cases the dielectrics are assumed to be generally lossy. Numerical results for these geometries are presented along with a discussion on the significance of these results.

II. Theoretical Analysis

Aperture admittance of a coaxial transmission line with a perfectly conducting flange of an infinite area, and opening into a layered dielectric composite media is formulated according to the work of Swift [20] which stemmed from the fundamental study developed by Levine and Papas [21]. Swift's formulation pertaining to a coaxial line antenna opening into a lossless dielectric covered ground plane is modified and expanded to take into account general N-layer media backed or unbacked with a conducting plate.

Fig. 1(a) shows the designated coordinate axis and the geometry of a coaxial transmission line with an infinite flange. Fig. 1(b) and (c) depicts the cross-sectional view of the line radiating into an N-layered media which is terminated by an infinite half-space and a perfectly conducting sheet, respectively. Each layer is assumed to be homogeneous and nonmagnetic with relative complex dielectric constant $\epsilon_{r_n} = \epsilon'_{r_n} - j\epsilon''_{r_n}$.

Manuscript received April 23, 1993; revised August 26, 1993. This work was supported in part by the Gates Rubber Company, Denver, CO.

The authors are with the Department of Electrical Engineering, Applied Microwave Nondestructive Testing Laboratory, Colorado State University, Fort Collins, CO 80523.

IEEE Log Number 9402372.

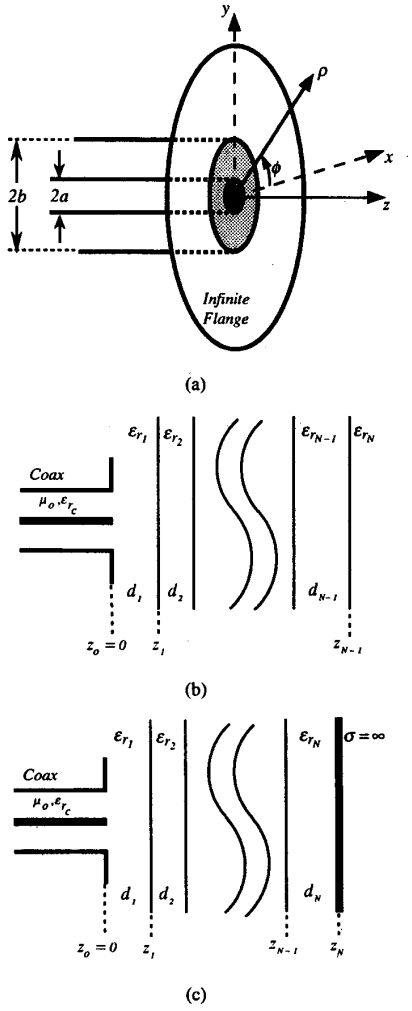

Fig. 1. (a) Coaxial transmission line of inner diameter $2a$ and outer diameter $2b$ opening onto a perfectly conducting infinite flange. (b) Cross section of coaxial line radiating into a layered media terminated into an infinite half-space. (c) Cross section of a coaxial line radiating into a layered media terminated into a perfectly conducting sheet.

With the dominant TEM mode incident on the aperture, the structure only supports H_ϕ, E_ρ, and E_z field components with no ϕ dependence. The external fields may be constructed using an electric or magnetic Hertz potential of the form

$$\overline{\Pi}_n(\rho, \phi, z) = \Pi_n^\phi(\rho, z)\hat{a}_\phi \tag{1}$$

where n denotes the layer number and $n = 0$ refers to the region internal to the coaxial line. The vector potential must satisfy the source-free Helmholtz wave equation in each region, and can be written as

$$\nabla^2\overline{\Pi}_n(\rho, \phi, z) + k_n^2\overline{\Pi}_n(\rho, \phi, z) = 0. \tag{2}$$

where $k_n = k_0\sqrt{\epsilon_{r_n}}$ is the complex propagation factor in the nth layer and k_0 is the free-space wave number. In terms of its scalar component, the above expression can be expressed as

$$\left[\frac{\partial^2}{\partial\rho^2} + \frac{1}{\rho}\frac{\partial}{\partial\rho} + \frac{\partial^2}{\partial z^2} + \left(k_n^2 - \frac{1}{\rho^2}\right)\right]\Pi_n^\phi(\rho, z) = 0. \tag{3}$$

Subsequently, the electric and magnetic field components satisfying the wave equation can be constructed from the vector potential formulation as

$$\begin{aligned}\overline{E}_n(\rho, z) &= \frac{1}{\epsilon_n}\nabla \times \overline{\Pi}_n(\rho, \phi, z) \\ &= \left[-\frac{1}{\epsilon_n}\frac{\partial\Pi_n^\phi}{\partial z}\right]\hat{a}_\rho + \left[\frac{1}{\epsilon_n}\frac{1}{\rho}\frac{\partial}{\partial\rho}(\rho\Pi_n^\phi)\right]\hat{a}_z\end{aligned} \tag{4}$$

$$\begin{aligned}\overline{H}_n(\rho, z) &= -\frac{1}{j\omega\mu_0\epsilon_n}(k_n^2 + \nabla\nabla\cdot)\overline{\Pi}_n(\rho, \phi, z) \\ &= j\omega\Pi_n^\phi\hat{a}_\phi.\end{aligned} \tag{5}$$

The solution of (3) can be written in terms of Hankel integral transforms of the form

$$\Pi_n^\phi(\rho, z) = \int_0^\infty \mathcal{R}\tilde{\Pi}_n^\phi(\mathcal{R}, z)J_1(\mathcal{R}\rho)\,d\mathcal{R} \tag{6a}$$

where

$$\tilde{\Pi}_n^\phi(\rho, z) = \int_0^\infty \rho\Pi_n^\phi(\rho, z)J_1(\mathcal{R}\rho)\,d\rho. \tag{6b}$$

$\mathcal{R}$ is a transformation variable denoting radial wave number. The notation $\sim$ represents the transformation and J_1 is Bessel function of the first kind and of order one. Substituting (6a) into (3) and using the orthogonal Bessel eigenfunctions properties and Dirac delta function Bessel integral representation [22] results in the following one-dimensional wave equation

$$\left(\frac{\partial^2}{\partial z^2} + k_{z_n}^2\right)\tilde{\Pi}_n^\phi(\mathcal{R}, z) = 0 \tag{7}$$

where

$$k_{z_n} = \sqrt{k_n^2 - \mathcal{R}^2},$$

and it is chosen such that $\mathrm{Re}\{k_{z_n}\} \geq 0$ and $\mathrm{Im}\{k_{z_n}\} \leq 0$. Next, one may construct the solutions of (7) for $z > 0$ in terms of standing and traveling waves as

$$\tilde{\Pi}_n^\phi(\mathcal{R}, z) = \mathcal{A}_n^+(\mathcal{R})e^{-jk_{z_n}z} + \mathcal{A}_n^-(\mathcal{R})e^{jk_{z_n}z}$$

Region bounded (8a)

$$\tilde{\Pi}_n^\phi(\mathcal{R}, z) = \mathcal{A}_n^+(\mathcal{R})e^{-jk_{z_n}z}$$

Region unbounded in $+z$ dir (8b)

Consequently, with the aid of (4) and (5) similar solutions may be constructed for the transformed field components as

$$\tilde{\mathcal{E}}_n^\rho(\mathcal{R}, z) = \frac{jk_{z_n}}{\epsilon_n}[\mathcal{A}_n^+(\mathcal{R})e^{-jk_{z_n}z} - \mathcal{A}_n^-(\mathcal{R})e^{jk_{z_n}z}] \tag{9}$$

$$\tilde{\mathcal{H}}_n^\phi(\mathcal{R}, z) = j\omega[\mathcal{A}_n^+(\mathcal{R})e^{-jk_{z_n}z} + \mathcal{A}_n^-(\mathcal{R})e^{jk_{z_n}z}]. \tag{10}$$

In accordance with (8b) the second term inside these brackets vanishes for an unbounded layer (i.e., in $+z$ direction). Next, the boundary conditions may be written in general form as

$$\text{For } 0 \leq n \leq N-1, \quad \begin{cases}\tilde{\mathcal{E}}_n^\rho(\mathcal{R}, z = z_n) = \tilde{\mathcal{E}}_{n+1}^\rho(\mathcal{R}, z = z_n) \\ \tilde{\mathcal{H}}_n^\phi(\mathcal{R}, z = z_n) = \tilde{\mathcal{H}}_{n+1}^\phi(\mathcal{R}, z = z_n)\end{cases} \tag{11a}$$

$$\tilde{\mathcal{E}}_n^{\rho}(\mathcal{R},\, z = z_N) = 0 \tag{11b}$$

where

$$z_n = \sum_{i=1}^{n} d_i, \begin{cases} 1 \le n \le N-1 \\ \quad N\text{th layer unbounded in } +z \text{ dir.} \\ 1 \le n \le N \\ \quad N\text{th layer backed by conducting sheet.} \end{cases} \tag{12}$$

With the dominant TEM mode incident on the aperture, the fields in this region, $z \le 0$ and $a \le \rho \le b$, can be written in terms of the incident and reflected wave as [23]

$$E_0^{\rho}(\rho,\, z) = \frac{A_0}{\rho}(e^{jk_c z} + Re^{-jk_c z}) \tag{13}$$

$$H_0^{\phi}(\rho,\, z) = \frac{Y_c A_0}{\rho}(e^{jk_c z} - Re^{-jk_c z}) \tag{14}$$

with

$$k_c = k_0\sqrt{\epsilon_{r_c}}, \quad \text{and} \quad Y_c = Y_0\sqrt{\epsilon_{r_c}},$$

where ϵ_{r_c} is the permittivity of the dielectric filling inside the coaxial line. $R = \Gamma e^{j\Phi}$ is the complex reflection coefficient, and Y_0 is the characteristic admittance of free-space.

To construct a solution for the aperture E-field in terms of the internal field quantities, one can take the integral Hankel transform of both sides of (13) at $z = 0$ as

$$\int_0^{\infty} E_0^{\rho}(\rho,\, z=0) J_1(\zeta\rho)\rho d\rho = \int_0^{\infty} \frac{A_0}{\rho}(1+R) J_1(\zeta\rho)\rho\, d\rho \tag{15}$$

and with the left-hand side term representing the Hankel transform of the aperture E-field, the right-hand side may then be evaluated over the aperture $a \le \rho \le b$, resulting in

$$\tilde{\mathcal{E}}_0^{\rho}(\mathcal{R}) = -A_0(1+R)\frac{J_0(\mathcal{R}b) - J_0(\mathcal{R}a)}{\mathcal{R}}. \tag{16}$$

Next, the continuity of power flow across the aperture required by Poynting's theorem is enforced over the aperture cross section S. Subsequently, application of Parseval's theorem for the integral transforms renders an equivalent relation for the complex conjugate of power flow in terms of the Hankel transform of the field components [22],

$$\begin{aligned} P^* &= \frac{1}{2}\int\int_S [\overline{E}^*(\rho,\, z) \times \overline{H}(\rho,\, z)] \cdot \hat{a}_z \rho\, d\rho d\phi \\ &= \int_{\mathcal{R}=0}^{\infty} \{\tilde{\mathcal{E}}^{\rho}(\mathcal{R},\, z)\}^* \tilde{\mathcal{H}}_{\phi}(\mathcal{R},\, z)\mathcal{R}\, d\mathcal{R}. \end{aligned} \tag{17}$$

From the above results, the outward power flow from the aperture, $z = 0$ and $a \le \rho \le b$, using (13) and (14) can be evaluated as

$$\vec{P}_{z=0}^{*} = \pi Y_c |A_0|^2 (1+R)^*(1-R)^* \ln\left(\frac{b}{a}\right) \tag{18}$$

where the arrow denotes the direction of flow (consistent with z-direction in Fig. 1). Similarly, the complex conjugate of power flow inward from layer one, at the aperture cross section as

$$\begin{aligned} \overleftarrow{P}_{z=0}^{*} &= \pi \int_0^{\infty} \{\tilde{\mathcal{E}}_1^{\rho}(\mathcal{R},\, z=0)\}^* \tilde{\mathcal{H}}_1^{\phi}(\mathcal{R},\, z=0)\mathcal{R}\, d\mathcal{R} \\ &= \pi \int_0^{\infty} \left|\tilde{\mathcal{E}}_0^{\rho}(\mathcal{R},\, z=0)\right|^2 \mathcal{F}(\mathcal{R})\mathcal{R}\, d\mathcal{R} \end{aligned} \tag{19}$$

where in the above equation the transform of the magnetic field component in region 1 is replaced with its equivalent expression. Function $\mathcal{F}(\mathcal{R})$, relating $\tilde{\mathcal{E}}_0^{\rho}(\mathcal{R},\, z)$ and $\tilde{\mathcal{H}}_1^{\phi}(\mathcal{R},\, z)$ results from enforcement of boundary conditions of (11) in the layered media and at the aperture. Equating (18) and (19) and substituting (16) for the transform of the aperture field allows construction of the normalized (with respect to characteristic admittance of the coaxial line) terminating aperture admittance. Consequently, using the normalization parameter $\zeta = (\mathcal{R}/k_0)$ the complex aperture admittance may be written as

$$\begin{aligned} y_s = g_s + jb_s &= \frac{1-R}{1+R} \\ &= \frac{\epsilon_{r_1}}{\sqrt{\epsilon_{r_c}}\ln\left(\frac{b}{a}\right)} \int_0^{\infty} \frac{[J_0(k_0\zeta b) - J_0(k_0\zeta a)]^2}{\zeta} \mathcal{F}(\zeta)\, d\zeta \end{aligned} \tag{20}$$

where g_s and b_s are the normalized aperture conductance and susceptance and R is the complex reflection coefficient. Consequently, enforcement of boundary conditions renders

$$\mathcal{F}(\zeta) = \frac{1}{\sqrt{\epsilon_{r_1} - \zeta^2}}\left(\frac{1+\rho_1}{1-\rho_1}\right) \tag{21}$$

For an N-layer media, ρ_1 may be calculated from the following recurrence relations. For $i = 1, 2, \cdots N-1$

$$\rho_i = \frac{1 - \kappa_i\beta_{i+1}}{1 + \kappa_i\beta_{i+1}} e^{-j2k_0 z_i\sqrt{\epsilon_{r_i} - \zeta^2}} \tag{22a}$$

where

$$\kappa_i = \frac{\epsilon_{r_i}}{\epsilon_{r_{i+1}}} \frac{\sqrt{\epsilon_{r_{i+1}} - \zeta^2}}{\sqrt{\epsilon_{r_i} - \zeta^2}} \tag{22b}$$

and

$$\beta_{i+1} = \frac{1 - \rho_{i+1}e^{j2k_0 z_i\sqrt{\epsilon_{r_{i+1}} - \zeta^2}}}{1 + \rho_{i+1}e^{j2k_0 z_i\sqrt{\epsilon_{r_{i+1}} - \zeta^2}}} \tag{22c}$$

and with z_i given by (12). For $i = N$,

$$\rho_N = \begin{cases} 0 \\ \quad N\text{th layer } \infty \text{ in } +z \text{ dir.} \\ e^{-j2k_0 z_N\sqrt{\epsilon_{r_N} - \zeta^2}} \\ \quad N\text{th layer terminated into a conducting sheet.} \end{cases} \tag{22d}$$

The above calculations must start from $i = N-1$ and carried out backward to $i = 1$. The value of ρ_N is chosen from (22d) depending on whether the Nth medium is an infinite half-space or is of finite thickness terminated into a conducting sheet.

Since many practical applications may be encompassed by a two-layer case, the explicit form of $\mathcal{F}(\zeta)$ for $N = 2$ in Fig. 1(b) and (c) is given next. For the geometry of Fig. 1(b)

where the second layer is infinite in $+z$ direction, recurrence relations of (22) result in the following simplified expression

$$\mathcal{F}(\zeta) = \frac{1}{\sqrt{\epsilon_{r_1} - \zeta^2}} \left[\frac{\kappa_1 + j \tan\left(k_0 d_1 \sqrt{\epsilon_{r_1} - \zeta^2}\right)}{1 + j\kappa_1 \tan\left(k_0 d_1 \sqrt{\epsilon_{r_1} - \zeta^2}\right)} \right] \quad (23)$$

where

$$\kappa_1 = \frac{\epsilon_{r_2}}{\epsilon_{r_1}} \frac{\sqrt{\epsilon_{r_1} - \zeta^2}}{\sqrt{\epsilon_{r_2} - \zeta^2}}.$$

Similarly, for the case shown in Fig. 1(c) and with $N = 2$, the procedure results in the following expression for $\mathcal{F}(\zeta)$ for the case of termination a conducting sheet

$$\mathcal{F}(\zeta) = \frac{j}{\sqrt{\epsilon_{r_1} - \zeta^2}} \cdot \left[\frac{\tan\left(k_0 d_1 \sqrt{\epsilon_{r_1} - \zeta^2}\right) \tan\left(k_0 d_2 \sqrt{\epsilon_{r_2} - \zeta^2}\right) - \kappa_1}{\kappa_1 \tan\left(k_0 d_1 \sqrt{\epsilon_{r_1} - \zeta^2}\right) + \tan\left(k_0 d_2 \sqrt{\epsilon_{r_2} - \zeta^2}\right)} \right]. \quad (24)$$

Consequently, substitution of (23) or (24) inside (20) will render the desired terminating aperture admittance solution for the $N = 2$ cases addressed here.

III. Verification and Implications of Numerical Results

To examine the validity and significance of the formulation presented here, a series of numerical simulations for the two-layer media are presented next. Two basic geometries are considered namely; a finite thickness dielectric layer backed by free-space and a two-layer media backed by a conducting sheet. When the thickness of layer 1 in the former case is set equal to zero, the aperture admittance expression of (20) in conjunction with (23) simplifies to that reported in [21]. Moreover, when the thickness of the dielectric layer in both cases are increased such that it constitutes an infinite half-space, once again one should arrive at the same results.

It should be noted that for the case of lossless ($\epsilon_r'' = 0$) layered media admittance expression given by (20) will encounter poles on the real axis along the path of integration, requiring contour integral techniques to carry out the integration. This problem, however, is not in the scope of this work since only generally lossy materials are of interest, in which case the poles move off the real axis and the integrand becomes smooth. In this case numerical integration routines such as Gauss–Legendre method [24], [25] may be readily employed.

In the numerical simulations presented here the calculated parameters in view of (20) are the experimentally measurable quantities of phase Φ of the complex reflection coefficient $R = \Gamma e^{j\Phi}$ and the return loss $RL = 20\log(1/\Gamma)$. The dielectric filling of the coaxial line in all cases is Teflon with $\epsilon_{r_c} = 2.07$. The real part of the complex dielectric constant of the medium is arbitrarily chosen to be $\epsilon_r' = 10$ and its loss tangent ($\tan\delta = \epsilon_r''/\epsilon_r'$) is varied between 0.01 and 1.0. These values are in the range of variety of synthetic rubber products and coating type materials on top of conducting sheets. First the effect of dielectric thickness is examined as shown in Fig. 2(a) and (b) at frequency of 5 GHz. It should be pointed out that by keeping $k_0 a$ and $r = b/a$ constant

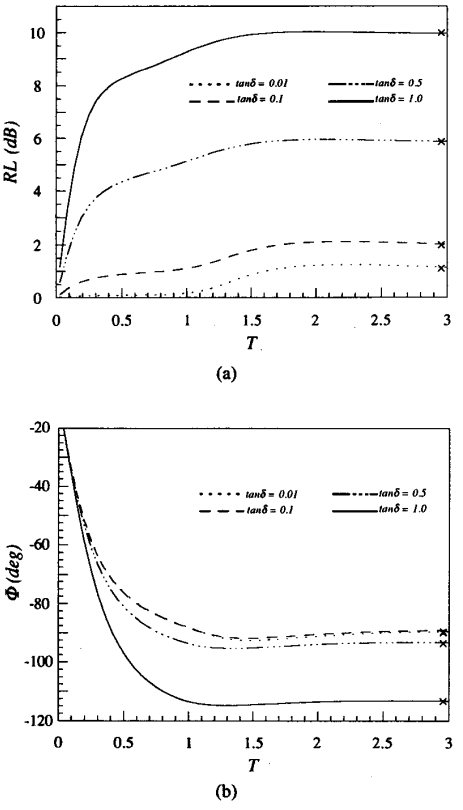

Fig. 2. (a) Return loss and (b) phase versus slab thickness normalized with respect to outer radius of the coaxial line. $\epsilon_{r_1}' = 10$, $\epsilon_{r_2}' = 1$ (air), frequency $f = 5$ GHz.

the same set of plots may apply to various coax dimensions and operating frequencies. The frequency range used in the simulations here is chosen below cutoff which is determined by the coax dimension. This is done to further justify the validity of disregarding higher order mode propagation inside the coaxial line. For these plots the dielectric slab thickness is normalized with respect to the coaxial line outer radius $T = d_1/(ar)$. This notation gives information about the ratio of the outer and inner conductor, as well as the absolute dimension of a or b. Fig. 2(a) and (b) displays a series of graphs for the return loss and phase of the complex reflection coefficient of a single layer terminated into an infinite free-space medium. This geometry may be deduced from Fig. 1(b) with $N = 2$ and $\epsilon_{r_2} = 1$. The normalized slab thickness is increased to ultimately approach that of an infinite half-space case. The points marked with $\times$ on these plots (Figs. 2 and 3) are calculated values using the infinite half-space formulation given in [21]. Clearly, there is a good agreement between these results. As expected, the response for the material with higher loss flatens out faster both for the return loss and phase. From Fig. 2(b) one may infer that the phase response does not change substantially below a certain value (e.g., $\tan\delta < 0.1$). Such curves (calculations) may be used to predict the "infinite" thickness for a given dielectric material for a specific operating frequency and coax dimensions. For the dielectric materials

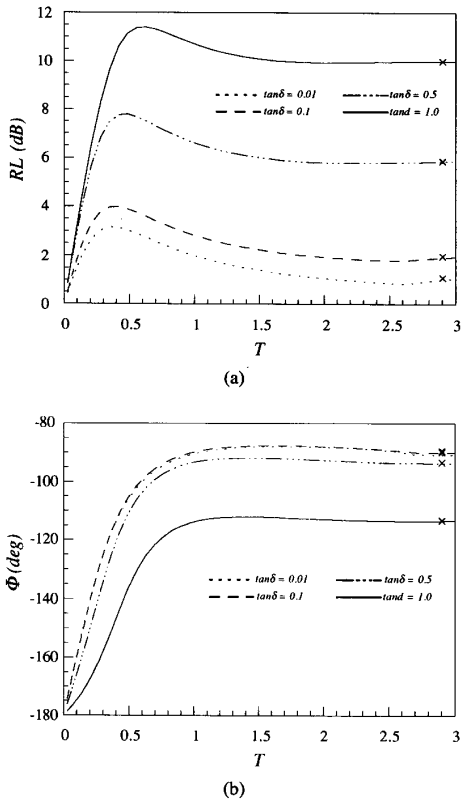

Fig. 3. (a) Return loss and (b) phase versus normalized thickness of the conductor backed slab. $\epsilon'_{r_1} = 10$, frequency $f = 5$ GHz.

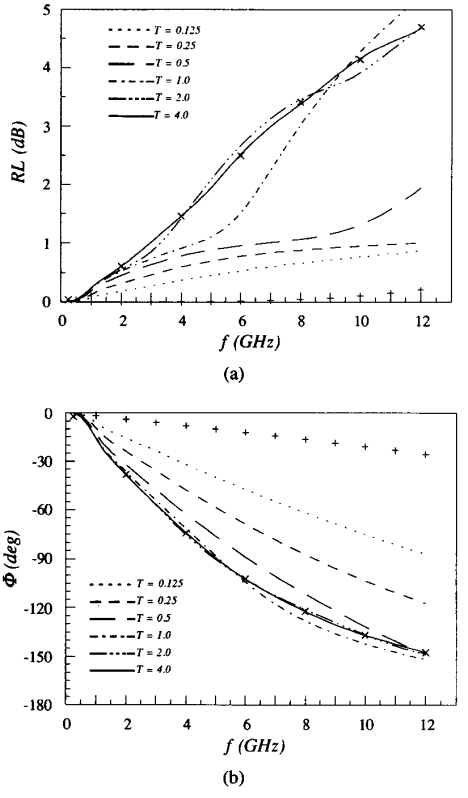

Fig. 4. (a) Return loss and (b) phase versus frequency for different thicknesses normalized with respect to outer radius of the coaxial line. $T = d_1/(ar)$, $r = b/a$, $\epsilon'_{r_1} = 10$, $\tan\delta_1 = 0.1$, $\epsilon_{r_2} = 1$ (air). × denotes points calculated for infinite dielectric, and + for air half-space.

used to calculate Fig. 2(b), it is evident that at this frequency for normalized thicknesses below 1.5, phase information may be used to accurately estimate material thickness. This observation suggests the possibility of utilization of coaxial sensors for accurate thickness measurement of thin dielectric sheets.

Fig. 3(a) and (b) shows the results for the case when the infinite half-space of air is replaced with a conducting sheet. Once more, crosses represent calculated results for infinitely thick sample [21]. In this case the return loss and phase reach to the valve infinite half-space for smaller values of T compared to the previous case. This is due to the two-way transmission through the dielectric. Conversely, as the thickness approaches zero, the return loss and phase values reach those of a short circuited coaxial line as expected. It can be observed from Figs. 2 and 3 that unlike open ended waveguide radiators [17], coaxial sensors in general seem to be less sensitive to small variations of complex permittivity for lossy materials.

Fig. 4(a) and (b) shows the return loss and phase as a function of frequency again for the case of a single slab of finite thickness terminated into an infinite free-space medium. The results are shown for dielectric with $\epsilon'_r = 10$ and $\tan\delta = 0.1$ for several different normalized slab thicknesses $T = d_1/(ar)$. The points marked with × and + on these plots are calculated using infinite half-space formulation [21] for the case of dielectric with the same properties and free-space, respectively. For small thickness the plots follow the trend of free-space curve. However, when the thickness increases the curves begin to oscillate around the infinite dielectric half-space curve. From Fig. 4(a) and (b) it may be concluded that normalized thickness $T = 4$ and greater constitute infinite half-space.

Subsequently, Fig. 5(a) and (b) shows the return loss and phase for the case of one layer being terminated into a conducting sheet with all the other parameters kept the same as the previous case. Comparison of Fig. 5(a) with its counterpart Fig. 4(a) displays a smoother response for this case which is attributed to stronger reflections at the dielectric/conducting interface. Subsequently, this effect at high enough frequencies gives rise to the phase transition for the thinnest slab shown in Fig. 5(b). These graphs also indicate the fact that once the slab's electrical thickness is large enough the response becomes independent of slab thickness and similar to that of infinite half-space media (marked with crosses).

Fig. 6(a) and (b) depicts return loss and phase versus frequency for two-layer conductor backed media. These plots attempt to demonstrate the potential of detecting a disbonded layer in such composites. Different curves pertain to different thicknesses of the second layer d_2 (i.e., different disbonds). The calculation parameters for this case are $a = 1.18$ mm, $b = 3.62$ mm, $\epsilon'_{r1} = 10$, $\tan\delta = 0.01$, $d_1 = 0.5$ mm,

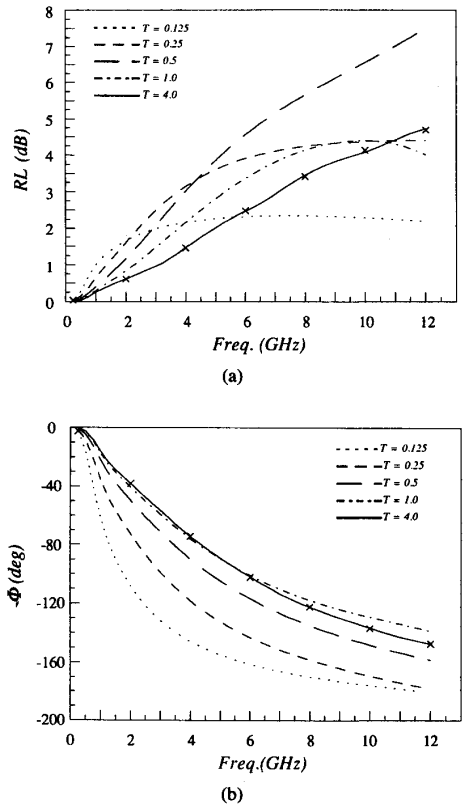

Fig. 5. (a) Return loss and (b) phase versus frequency for different normalized thicknesses of the conductor backed slab. $T = d_1/(ar)$, $r = b/a$, $\epsilon'_{r_1} = 10$, $\tan\delta_1 = 0.1$, and $\times$ denotes points calculated for infinite dielectric.

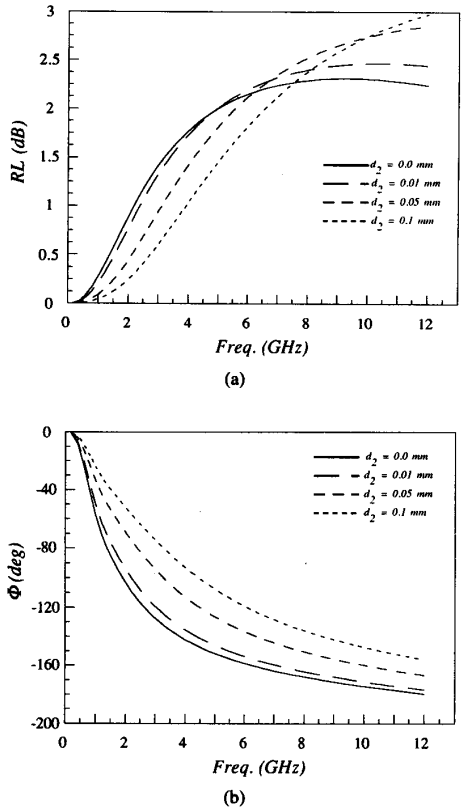

Fig. 6. (a) Return loss and (b) phase versus frequency for different disbonds, d_2, in a two-layer media backed by a conducting sheet. $\epsilon_{r_2} = 1$ (air), $\epsilon'_{r_1} = 10$, $\tan\delta_1 = 0.01$, $d_1 = 0.5$ mm, $a = 1.18$ mm, $b = 3.62$ mm.

and $\epsilon'_{r2} = 1$ (air disbond layer). Any increase in d_2 is compensated by a decrease in d_1, such that $d_1 + d_2$ is kept constant. From Fig. 6(a) and (b) it may be concluded that phase is more sensitive to the presence of disbond compared to return loss. For higher frequencies a disbonded layer in the order of a fraction of a millimeter may be easily detected. This demonstrates the ability to detect small disbonds when a dielectric layer is backed by a conductor (e.g., thermal barrier coating, paint, etc.).

IV. Conclusions

A general formulation for aperture admittance of an open-ended coaxial transmission line terminated by layered dielectric composite is presented. The fields are formulated with the aid of integral Hankel transforms. The terminating admittance is constructed by applying the complex Poynting's theorem to enforce the continuity of power flow across the aperture. A set of recurrence relations were provided allowing efficient construction of solutions for arbitrary multilayered geometries backed or unbacked with a conducting sheet. The numerical results presented pertained to specific practical cases of a two-layer generally lossy composite and two-layer composite backed by a conducting sheet. The theory was examined by comparison with a readily available infinite half-space model which had been experimentally verified. The formulation presented here may be used in many practical applications such as measurement of dielectric properties (or dimensions) of finite thickness dielectric materials, estimating equivalent "infinite thickness" of a given dielectric, modeling of field coupling into layered biological media in biomedical applications, examination of multilayered coating deposits on metals, and disbond detection in stratified dielectrics.

An important practical issue, when dealing with open-ended coaxial lines, is calibration. Conventionally, loads such as short circuit, open circuit, and a liquid with well known dielectric properties are used for measurement calibration of open-ended coaxial sensors. However, it is relatively difficult to provide a perfect short or even a perfect open circuit. Incorporation of thickness into the solution provides for a new alternative method for calibration of open-ended coaxial sensors. Slabs with known dielectric properties and different thickness may be used for calibration too. Airgap distance variation between the aperture and the slab in front of the sensor may also be used as a means of calibration. In both cases multiple calibration data points may be obtained rendering for a more precise calibration technique.

References

[1] M. Stuchly and S. Stuchly, "Coaxial line reflection methods for measuring dielectric properties of biological substances at radio and microwave

frequencies—A review," *IEEE Trans. Instrum. Meas.*, vol. IM-29, pp. 176–183, Sept. 1980.
[2] J. Mosig, J.-C. Besson, M. Gex-Farby, and F. Gardiol, "Reflection of an open-ended coaxial line and application to nondestructive measurement of materials," *IEEE Trans. Instrum. Meas.*, vol. IM-30, pp. 46–51, Mar. 1981.
[3] D. Misra, "A quasi-static analysis of open-ended coaxial lines," *IEEE Trans. Microwave Theory Tech.*, vol. MTT-35, pp. 925–928, Oct. 1987.
[4] T. Marsland and S. Evans, "Dielectric measurements with an open-ended coaxial probe," *IEE Proc.*, vol. 134, Pt.H, pp. 341–349, Aug. 1987.
[5] D. Misra, M. Chabra, B. Epstein, M. Mirotznik, and K. Foster, "Noninvasive electrical characterization of materials at microwave frequencies using an open-ended coaxial line: Test of an improved calibration technique," *IEEE Trans. Microwave Theory Tech.*, vol. 38, pp. 8–14, Jan. 1990.
[6] K. Staebel and D. Misra, "An experimental technique for *in vivo* permittivity measurement of materials at microwave frequencies," *IEEE Trans. Microwave Theory Tech*, vol. MTT-38, pp. 337–339, Mar. 1990.
[7] E. Burdette, F. Cain, and J. Seals, "*In vivo* probe measurement technique for determining dielectric properties at VHF through microwave frequencies," *IEEE Trans. Microwave Theory Tech.*, vol. MTT-28, pp. 414–426, Apr. 1980.
[8] M. El-Rayes and F. Ulaby, "Microwave spectrum of vegetation—Part I: Experimental observations," *IEEE Trans. Geosci. Remote Sensing*, vol. GE-25, pp. 541–549, Sept. 1987.
[9] R. Seaman, E. Burdete, and R. Dehaan, "Open-ended coaxial exposure device for applying RF/microwave fields to very small biological preparations," *IEEE Trans. Microwave Theory Tech.*, vol. 37, pp. 102–111, Jan. 1989.
[10] Y. Xu, R. Bosisio, and T. Bose, "Some calculation methods and universal diagrams for measurement of dielectric constants using open-ended coaxial probes," *IEE Proc. H*, vol. 138, pp. 356–360, Aug. 1991.
[11] T. Athey, M. Stuchly, and S. Stuchly, "Measurement of radio frequency permittivity of biological tissues with an open-ended coaxial-line: Part I," *IEEE Trans. Microwave Theory Tech.*, vol. MTT-30, pp. 82–86, Jan. 1982.
[12] "Measurement of radio frequency permittivity of biological tissues with an open-ended coaxial-line: Part II—Experimental results," *IEEE Trans. Microwave Theory Tech.*, vol. MTT-30, pp. 87–92, Jan. 1982.
[13] H. Zheng and C. Smith, "Permittivity measurements using a short open-ended coaxial probe," *IEEE Microwave Guided Wave Lett.*, vol. 1, pp. 337–339, Nov. 1991.
[14] S. Ganchev, N. Qaddoumi, D. Brandenburg, S. Bakhtiari, R. Zoughi, and J. Bhattacharyya, "Microwave diagnosis of rubber compounds," *IEEE Trans. Microwave Theory Tech.*, vol. 42, pp. 18–24, Jan. 1994.
[15] S. Bakhtiari, S. Ganchev, and R. Zoughi, "Open-ended rectangular waveguide for nondestructive thickness measurement and variation detection of lossy dielectric slabs backed by a conducting plate," *IEEE Trans. Instrum. Meas.*, vol. 42, pp. 19–24, Feb. 1993.
[16] "Microwave frequency optimization for accurate thickness or dielectric property monitoring of conductor backed composites," *Materials Eval.*, vol. 51, pp. 740–748, June 1993.
[17] S. Bakhtiari, N. Qaddoumi, S. Ganchev, and R. Zoughi, "Microwave noncontact examination of disbond and thickness variations in stratified composite media," *IEEE Trans. on Microwave Theory Tech.*, vol. 42, pp. 389–395, Mar. 1994..
[18] S. Fan, K. Staebel, and D. Misra, "Static analysis of an open-ended coaxial line terminated by layered media," *IEEE Trans. Instrum. Meas.*, vol. 39, pp. 435–437, Apr. 1990.
[19] L. Anderson, G. Gajda, and S. Stuchly, "Analysis of an open-ended coaxial line sensor in layered dielectrics," *IEEE Trans. Instrum. Meas.*, vol. IM-35, pp. 13–18, Mar. 1986.
[20] C. Swift, "Input admittance of a coaxial transmission line opening onto a flat, dielectric-covered ground plane," NASA Tech. Note D-4158, Sept. 1967.
[21] H. Levine and C. Papas, "Theory of circular diffraction antenna," *J. Appl. Phys.*, vol. 22, pp. 29–43, 1951.
[22] G. Arfken, *Mathematical Methods for Physicists.* New York: Academic, 1985.
[23] N. Marcuvitz, *Waveguide Handbook.* New York: McGraw-Hill, 1951, pp. 213–216.
[24] W. H. Press, B. P. Flannery, S. A. Teukolsky, and W. T. Vetterling, *Numerical Recipes.* Cambridge, England: Cambridge University Press, 1986.
[25] S.Ganchev, S. Bakhtiari, and R. Zoughi, "A novel numerical technique for dielectric measurement of generally lossy dielectrics," *IEEE Trans. Instrum. Meas.*, vol. 41, pp. 361–465, June 1992.

Sasan Bakhtiari (M'94), for a photograph and biography, see page 24 of the January issue of this TRANSACTIONS.

Stoyan I. Ganchev (M'92–SM'92), for a photograph and biography, see page 23 of the January issue of this TRANSACTIONS.

Reza Zoughi (M'87–SM'93), for a photograph and biography, see page 24 of the January issue of this TRANSACTIONS.